Binding Free Energy Calculations to Rationalize the Interactions of Huprines with Acetylcholinesterase

Érica C. M. Nascimento, Mónica Oliva, and Juan Andrés**

Departament de Química Física i Analítica, Universitat Jaume I, Av. de Vicent Sos Baynat, s/n 12071 Castellón, Spain

Corresponding author information:

Mónica Oliva: e-mail; oliva@uji.es; tel: +34964728088

Juan Andrés: e-mail: andres@uji.es; tel: +34964728083

ORCID: E.C.M. Nascimento 0000-0003-1365-177X; M. Oliva 0000-0001-6651-7852; J. Andrés 0000-0003-0232-3957

Abstract: In the present study, the binding free energy of a family of huprines with acetylcholinesterase (AChE) is calculated by means of the free energy perturbation method (FEP), based on hybrid quantum mechanics and molecular mechanics (QM/MM) potentials. Binding free energy calculations and the analysis of the geometrical parameters highlight the importance of the stereochemistry of huprines in AChE inhibition. Binding isotope effects (BIE) are calculated to unravel the interactions between ligands and the gorge of AChE. New chemical insights are provided to explain and rationalize the experimental results. A good correlation with the experimental data is found for a family of inhibitors with moderate differences in the enzyme affinity. The analysis of the geometrical parameters and interaction energy per residue reveals that Asp72, Glu199, and His440 contribute significantly to the network of interactions between active site residues, which stabilize the inhibitors in the gorge. It seems that a cooperative effect of the residues of the gorge determines the affinity of the enzyme for these inhibitors, where Asp72, Glu199, and His440 make a prominent contribution.

Formatat: Espanyol (Espanya)

Formatat: Espanyol (Espanya)

Codi de camp canviat

Formatat: Espanyol (Espanya)

Formatat: Espanyol (Espanya)

Codi de camp canviat

Codi de camp canviat

Formatat: Espanyol (Espanya)

Formatat: Espanyol (Espanya)

Formatat: Espanyol (Espanya)

Keywods: Huprines, binding free energy calculation, QM/MM, stacking interactions, binding isotope effect.

Acknowledgements

We thank Prof P. Camps, Prof. F.J. Luque, and Prof. D. Muñoz-Torrero for interesting comments on the paper. The authors acknowledge the financial support of the following agencies: Generalitat Valenciana for PrometeoII/2014/022, Ministerio de Economia y Competitividad, project CTQ2015-65207-P, Universitat Jaume I for project UJI-B2016-25. E.C.M. Nascimento is grateful to the Generalitat Valencia for Santiago Grisolia program 2011/040. We also wish to thank the Servei d'Informática, Universitat Jaume I, for the generous allocation of computer time.

Introduction

Alzheimer's disease (AD) is mainly characterized by the formation of deposits of extracellular amyloid plaques and the intraneuronal neurofibrillary tangles of hyperphosphorylated tau protein [1]. Modifications of several neurotransmitter systems have also been observed, with the most characteristic being the relatively selective loss of cholinergic neurons [1]. The depletion of cholinergic neurotransmission in the brain of AD patients gave rise to the cholinergic hypothesis of AD [2-4], which afforded the rational basis from which most of the currently approved anti-Alzheimer drugs have derived. Indeed, four out of the five approved drugs are inhibitors of the enzyme acetylcholinesterase (AChE). This enzyme is responsible for the hydrolysis of acetylcholine, and therefore its inhibition can restore the cholinergic transmission to some extent. Apart from the acetylcholinesterase inhibitors (AChEIs), memantine, a glutamate NMDA receptor antagonist, was also approved for AD treatment [5]. While a number of drug candidates deriving from other hypotheses, prominently the amyloid hypothesis, have not yet provided satisfactory results in clinical trials, AChEIs constitute the basis of AD treatment and the design of novel AChEIs is still an area of very intensive research.

Some AChEIs, such as rivastigmine [6], form covalent bonds with the Ser200 (*Torpedo californica* AChE numbering) residue of AChE, whereas most inhibitors, including the approved drugs tacrine [7], donepezil [8], and galantamine [9], block the active site of the enzyme through non-covalent reversible interactions. Prediction of the binding affinities of AChEIs can be very useful for the development of novel inhibitors. This is one of the great challenges of computational chemistry, and several methods have been applied in an attempt to obtain a reliable prediction of protein-ligand binding energies [10-12].

As far as AChE is concerned, several protocols have been used to estimate the binding affinity of numerous ligands [13-21]. Unfortunately, the methods with less computational cost were not always able to reproduce the experimental results [18]. Recently, we have published a paper where the binding free energy of some classical inhibitors of AChE was calculated, obtaining good results with an acceptable computational cost [22]. In that work, the ligands that were studied had quite different protein affinities. However, it is interesting to compare inhibitors with a similar inhibition constant. To verify if our protocol

is adequate in the latter circumstances, we have decided to apply it to a set of huprines, a known class of AChEIs, which feature similar characteristics and affinity.

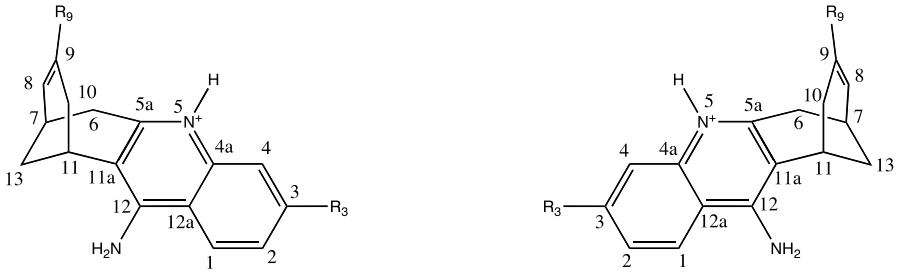

(+)-(7*R*,11*R*)-huprine (-)-(7*S*,11*S*)-huprine

R_3=Cl, R_9=Ethyl: HUX
R_3=Cl, R_9=Methyl: HUY
R_3=H, R_9=Ethyl: HUE
R_3=H, R_9=Methyl: HUM

Scheme 1 Schematic representation of the huprines considered in this study

Huprines are a group of tacrine-huperzine A hybrids that simultaneously feature the 4-aminoquinoline system of tacrine and the carbobicyclic bridged system of huperzine A [16,14,23,24]. These compounds are racemic species, which can be separated into their enantiomers (Scheme 1). The levorotatory enantiomers of these hybrid compounds ((-)-(7*S*,11*S*)-huprines) are far more active (eutomers) for AChE inhibition than the dextrorotatory forms (distomers), and the most active derivatives are those substituted at position 3 with a chlorine atom (Table 1) [16,14,23,21].

Huprine X binds to human AChE with an affinity 40-fold higher than that of donepezil, 180-fold higher than that of (-)-huperzine A, and 1200-fold higher than that of tacrine [19,23]. The simultaneous occupancy of the binding zone of tacrine and a part of the binding zone of (-)-huperzine A by huprines seems to be responsible for their high inhibitory potency [24]. Pharmacological studies have demonstrated that huprine X exhibits an agonistic action on muscarinic M_1 and nicotinic receptors [25,26]. Moreover, results obtained in efficacy studies in mice strongly suggest that treatment with huprine X improves the cognitive performance of the animals and induces some neurochemical changes which could contribute to the beneficial effects observed [27]. The outstanding pharmacological profile of huprines together with the work by Pang, Carlier and Han on tacrine dimers as dual binding

site AChE inhibitors inspired the synthesis of new heterodimeric compounds based on huprine, such as huprine-tacrine heterodimers or donepezil-huprine heterodimers, among others [24,21].

Table 1 AChE inhibitory activity (IC_{50} values, nM) and affinity (K_i values, nM) of the huprines considered in the study, for the racemic mixture, (-)-(7*S*,11*S*)-enantiomer and (+)-(7*R*,11*R*)-enantiomer. Data taken from Refs. ([16,14,23,21]).

Compound	R_3	R_9	IC_{50}rac (nM)	IC_{50}(-) (nM)	IC_{50}(+) (nM)	K_i (nM) [23]
HUX	Cl	Ethyl	2.77±0.75[a] [16] 0.67±0.05[b] [21]	1.30±0.26[a] [16] 0.27±0.02[b] [21]	402±36[a] [16] 6.30±0.50[b] [21]	0.026±0.002[b] [23]
HUY	Cl	Methyl	4.23±0.86[a] [16] 0.61±0.03 [21]	1.15±0.11[a] [16] 0.43±0.03[b] [21]	36.1±3.6[a] [16] 13.6±1.5[b] [21]	0.033±0.003[b] [23]
HUE	H	Ethyl	38.5±4[a] [16]	27.4±3.1[a] [14]	888±141[a] [14]	n.a.
HUM	H	Methyl	65±15[a] [16]	47.1±6.3[a] [14]	329±58[a] [14]	n.a.

[a] values determined from inhibition of bovine erythrocyte AChE, [b] values determined from inhibition of human AChE

As a continuation of the previous paper [22], here we present a study aimed at gaining an understanding of the binding process of huprines. Binding free energies are calculated by means of the alchemical free energy perturbation (FEP) method. FEP is a recognized method for the prediction of ligand binding poses and affinities [28,29]. The contributions of each residue of the gorge to the interaction energy between the inhibitors and the enzyme have been analyzed, and these results have been connected with the geometrical parameters obtained in our simulations. Finally, binding isotope effects [30] (BIE) have been calculated to further analyze interactions between ligands and the gorge of AChE.

Models and Methods

System setup

The system setup was performed following the same protocol used in our previous work on the classical AChE inhibitors [22]. In this way, we used the same structure for the protein and structural water molecules (PDB code 2C5G), and the coordinates of (-)-huprine X were put in the gorge by superimposing the AChE structure complexed with huprine X (PDB ID 1E66) using the DaliLite program [31]. All structural water molecules in the gorge, as well as the coordinates of residues Phe330 and Trp432, were replaced in the new coordinate systems according to the 1E66 pdb file. The root mean square deviation (RMSD) was 0.18 Å, and thus the structures obtained after superimposition were assumed to be suitable for this study. The other (-)-huprines-AChE systems were obtained after minor changes in positions 3 and/or 9 of (-)-huprine X. With regard to (+)-huprines, the initial coordinates for these systems were obtained after docking the corresponding (+)-huprines in the *Torpedo californica* AChE (TcAChE) 2C5G pdb file using the AutoDock 4.2 program [32]. The coordinates of Phe330 and Trp432 were also adjusted according to the 1E66 pdb file. Regarding the protonation state of the residues, the enzyme was modeled with neutral His440 and deprotonated Glu327 and Glu199. The standard ionization state at neutral pH was considered for the rest of the ionizable residues with the exception of Asp392 and Glu443, which were neutral, and His471, which was protonated, in accordance with our previous work [22] and in agreement with Wlodek and co-workers [13].

Hydrogen atoms were incorporated into the structure, and the energy minimization of these atoms was performed as implemented in the fDynamo library [33,34]. Next, 5 sodium counterions were added in optimal electrostatic positions around the protein (never closer than 10.5 Å to any atom and not less than 5 Å from another counterion, using a regular grid of 0.5 Å) so as to have a total charge equal to zero. Subsequently, the system was placed inside a previously relaxed box of water (100×100×100 $Å^3$). All water molecules within a distance of 2.8 Å from the protein were removed.

In the present study, all calculations were performed with the hybrid Quantum Mechanics/Molecular Mechanics (QM/MM) method as implemented in the fDynamo library [33,34]. The huprines were treated using the semi-empirical AM1 method [35], and the rest of the system (protein and solvent) were described using OPLS-AA [36] and TIP3P [37]

force fields, respectively. After energy minimization of the systems, 300 ps of AM1/MM molecular dynamics (MD) simulations were carried out, where all atoms were free to move. In order to reduce the computational cost of the calculations, these simulations were followed by 1 ns AM1/MM MD, where the residues and water molecules at a distance of 25 Å or greater from the OG atom of the residue Ser200, were kept frozen. In both cases, Langevin-Verlet (NVT) MD were performed at 300 K with a time step of 1 fs, applying periodic boundary conditions and cutoff using a switching scheme within a radius ranging from 14 to 16 Å.

Inhibitor-solvent systems were also required to compute the AChE-ligands binding free energy, and thus several systems were built by placing each inhibitor in the pre-relaxed box of water. AM1/MM MD simulations for the inhibitor-solvent system were also conducted. First the inhibitor-solvent system simulations were performed considering all atoms to be free for 100 ps. Subsequently, 300 ps of AM1/MM MD were carried out where all water molecules at a distance of 25 Å or greater from the carbon atom that holds the amine group were frozen, and the equilibration simulation time was 300 ps.

Alchemical Free Energy Perturbation (FEP) Method

The starting structures in FEP calculations were the equilibrated AChE-huprine and water-huprine systems described in the previous section. In order to evaluate the huprine-protein binding free energy, a series of AM1/MM MD simulations have been carried out at the gorge and in the box of solvent, introducing the parameters λ and γ into the electrostatic and van der Waals QM/MM interaction terms, as shown in Equation 1.

$$E_{QM/MM}(\lambda,\gamma) = \left\langle \Psi \mid \hat{H}_0 \mid \Psi \right\rangle + \lambda \left(\sum \left\langle \Psi \left| \frac{q_{MM}}{r_{e,MM}} \right| \Psi \right\rangle + \sum\sum \frac{Z_{QM}\, q_{MM}}{r_{QM,MM}} \right) + \gamma E^{vdW}_{QM/MM} + E_{MM} \quad (1)$$

In this equation, λ changes smoothly between the values of 1 and 0. The λ parameter scales the electrostatic interaction term between the MM and QM atoms, which affects both the interaction between electrons and MM atoms, and the interaction between QM nuclei and MM atoms. The parameter λ equal to 1 corresponds to a full MM charge–QM atoms interaction, whereas a value of λ equal to 0 represents no electrostatic interaction with the

force field. The γ values are also comprised between 1 and 0 (once the electrostatic charges of the ligand in the QM region are annihilated); when it is equal to 1 it corresponds to a full QM/MM van der Waals interaction, while a value equal to 0 refers to no van der Waals interaction with the force field [38].

A total of 50 windows were used to evaluate the electrostatic interaction energy term, from λ= 1 (full interaction) to λ= 0 (no electrostatic interaction), in steps (δλ) of 0.02. The same number of windows were used to calculate the van der Waals energy interaction term, from γ= 1 (full interaction) to γ= 0 (no interaction) in steps (δγ) of 0.02. A total of 10 ps of relaxation followed by 100 ps of production of AM1/MM MD simulation were performed using the NVT ensemble at the reference temperature of 300 K. This simulation time provided suitable results in previous papers based on the same protein, where the consistence of the free binding energy as a function of the simulation time was analyzed [22], as well as on other proteins [38,39]. The calculation of free-energy differences of two consecutive windows of the two stages, annihilation of charges and the van der Waals parameters, was performed by means of the FEP method. The total Helmholtz free energy variation (ΔF) was calculated through the sum of all the windows covering the full transformation from the initial to the final states. This procedure is carried out in two steps, as represented in Equations 2 and 3 [38]:

$$\Delta F_{QM/MM}^{elect} = -\frac{1}{\beta}\sum_{\lambda=1} \ln\left\langle e^{-\beta\left[E(\lambda_{i+1})-E(\lambda_i)\right]}\right\rangle_{\lambda_i} \quad (2)$$

$$\Delta F_{QM/MM}^{vdW} = -\frac{1}{\beta}\sum_{\gamma=0} \ln\left\langle e^{-\beta\left[E(\gamma_{i+1})-E(\gamma_i)\right]}\right\rangle_{\gamma_i} \quad (3)$$

The thermodynamic cycle used to compute the binding free energy of enzyme-inhibitors by alchemical FEP methods is presented in Scheme 2. In this way, free energy is calculated by applying Equations 2 and 3, in water (W) and in the enzyme (E)

$$\Delta F = \Delta F_E - \Delta F_W \quad (4)$$

This calculation is performed in two steps yielding the electrostatic and van der Waals terms, ΔF_{elec} and ΔF_{wdW}. Finally, the total binding free energy is obtained by adding the two terms:

$$\Delta F_{bind} = \Delta F_{elec} + \Delta F_{vdW} \qquad (5)$$

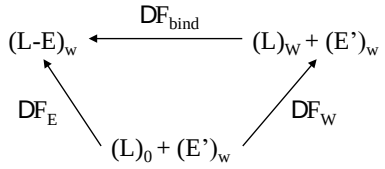

Scheme 2 Thermodynamic cycle to compute enzyme-huprine binding free energies. E is the enzyme with huprine (L) in its binding site, E' is the apo form of the enzyme, and $(L)_0$ is the ligand in gas phase

Interaction Energy per Residue

The interaction energy between the huprine and the protein is calculated as the difference between the QM/MM energy and the energies of the non-interacting QM and MM subsystems for the same system geometry. This interaction energy can be decomposed in a sum over the residues, the residue (i) is turned on and off, thus obtaining the contribution of each of them to the interaction energy as expressed in Equation (6):

$$E^{Int}_{QM/MM,i} = E^{elect}_{QM/MM,i} + E^{vdW}_{QM/MM,i}$$

$$= \sum_{MM \in i} \left[\left\langle \Psi \left| \frac{q_{MM}}{r_{e,MM}} \right| \Psi \right\rangle + \sum_{QM} \frac{Z_{QM} q_{MM}}{r_{QM,MM}} \right] \qquad (6)$$

$$+ \sum \sum 4\varepsilon_{QM.MM} \left[\left(\frac{\sigma_{QM,MM}}{r_{QM,MM}} \right)^{12} - \left(\frac{\sigma_{QM,MM}}{r_{QM,MM}} \right)^{6} \right]$$

The average interaction energy per residue has been obtained using the 1ns AM1/MM MD simulations for each huprine-AChE system. The structures of the last 500 ps have been considered for these calculations.

Binding Isotope Effects (BIEs)

Binding isotope effects (BIEs) can be a useful tool to identify important non-bonding interactions occurring during the binding of the inhibitor to the active site. Changes in normal-mode force constants surrounding the isotopic substitution, between inhibitor dissolved in water and inhibitor in the active site of the enzyme, give rise to a binding preference for a light or a heavy isotope in the bound state and hence a measurable BIE [30].

Considering the binding process of an inhibitor, from solution to the formation of the inhibitor-enzyme complex, BIE would be defined as the ratio between the binding equilibrium constant of the light (L), or naturally abundant, isotope species and the heavy (H), or isotopically substituted, one:

$$BIE = \frac{K_L}{K_H} \qquad (7)$$

BIEs can also be expressed in terms of the binding free energy of the light and heavy species, considering the relationship between the equilibrium constant and the binding free energy:

$$BIE = e^{-(\Delta G_L + \Delta G_H)/RT} \qquad (8)$$

where ΔG_L and ΔG_H are the binding free energies for the light and heavy isotopomers, respectively, R is the universal gas constant, and T is the temperature. Considering the definition of free energy of a state, as a function of the internal energy, the total partition function and the zero point vibrational energy, the binding isotope effect can be calculated using equation (9):

$$BIE = \frac{\left(\frac{Q_e}{Q_w}\right)_L}{\left(\frac{Q_e}{Q_w}\right)_H} e^{-1/RT\left(\Delta ZPE_L - \Delta ZPE_H\right)} \qquad (9)$$

In equation (9), Q_e is the total partition function (the product of translational, rotational, and vibrational partition functions) for the inhibitor in the enzyme, and Q_w is the total partition function for the inhibitor in water. ΔZPE_L and ΔZPE_H are the differences in zero point vibrational energies from water to the gorge of AChE, for the inhibitor with the light and heavy isotope, respectively.

BIEs were calculated by selecting eleven structures from the 1ns AM1/MM MD simulation for each AChE-huprine system, and eleven structures from the 300 ps AM1/MM MD simulation for each huprine in solution. These structures were obtained from the last 200 ps of these simulations.

Results and discussion

FEP results

The huprine-AChE binding free energies (ΔF_{bind}**)** and their decomposition into electrostatic and van der Waals terms computed from the FEP method are reported in Table 2. The electrostatic terms of protein-ligand ($\Delta F_{elec\text{-}E}$) and water-ligand ($\Delta F_{elec\text{-}W}$) are calculated by means of equation 2, and the corresponding van der Waals terms of protein-ligand ($\Delta F_{vdW\text{-}E}$) and water-ligand ($\Delta F_{vdW\text{-}W}$) systems are calculated using equation 3. The differences between electrostatic terms in the enzyme and water provide the electrostatic contribution to the binding process (ΔF_{elec}), which ranges from -17.04 to -25.21 kcal·mol^{-1}, for the least and most potent inhibitors, respectively. For the (-)-(7*S*,11*S*)-huprines this term correlates with the binding free energy, whereas for the (+)-(7*R*,11*R*)-huprines the value is substantially lower, around -17.5 kcal·mol^{-1}, and no trends are observed. Regarding the differences in van der Waals terms in the protein and in solution, the van der Waals contribution (ΔF_{vdW}) to the binding energy is always smaller than the corresponding electrostatic one for each inhibitor. However, the van der Waals term is not negligible and contributes significantly to the binding free energy (Figure 1). This contribution accounts for around 45% of the total binding energy in most systems, except for (-)-HUY and (+)-HUM systems, where this term represents 38% and 40% of the total binding free energy, respectively. It is interesting to note that for most inhibitors, the value of ΔF_{vdW} is between -15 and -17 kcal·mol^{-1}, but for (-)-HUX (the most

potent inhibitor) ΔF_{vdW} is -19.58 kcal·mol^{-1}, and for the less effective inhibitors the value is close to -12.5 kcal·mol^{-1}.

Table 2 Electrostatic (ΔF_{elec}) and van der Waals (ΔF_{vdW}) terms of the water-ligand ($_{-W}$) and protein-ligand ($_{-E}$) interaction free energy, and differences in interaction between the binding site of the protein and water (ΔF_{elec}, ΔF_{vdW}) and the binding free energy (ΔF_{bind}). Values in kcal mol^{-1}

	W(water)		**E(Enzyme)**		**ΔF**		**ΔF_{bind}**
Ligand	ΔF_{elec-W}	ΔF_{vdW-W}	ΔF_{elec-E}	ΔF_{vdW-E}	ΔF_{elec}	ΔF_{vdW}	*calculated*
(-)-HUX	-19.51	-23.31	-44.72	-42.89	-25.21	-19.58	**-44.79**
(-)-HUY	-20.82	-23.34	-45.58	-38.36	-24.76	-15.02	**-39.78**
(-)-HUE	-19.32	-23.23	-40.49	-40.12	-21.17	-16.89	**-38.06**
(-)-HUM	-19.56	-23.03	-40.31	-38.99	-20.75	-15.96	**-36.71**
(+)-HUE	-19.68	-23.73	-37.02	-39.66	-17.34	-15.93	**-33.27**
(+)-HUX	-19.35	-22.58	-36.96	-38.00	-17.61	-15.42	**-33.03**
(+)-HUM	-17.81	-21.62	-35.81	-33.75	-18.00	-12.13	**-30.13**
(+)-HUY	-21.00	-23.27	-38.04	-35.82	-17.04	-12.55	**-29.59**

The affinity of (-)-huprines for AChE is considerably greater than that of the (+)-huprine, in agreement with the experimental data (Table 1) [16,14,21]. Figure 2 shows the correlation between our results and experimental values of binding free energy, corresponding to the IC_{50} values determined from inhibition of bovine erythrocyte AChE [16,14]. As can be seen in the figure, there are some discrepancies between these experimental data and our results. According to the FEP results the most potent inhibitor is (-)-HUX, but the experimental IC_{50} for (-)-HUX and (-)-HUY are 1.30 ± 0.26 and 1.15 ± 0.11 nM, respectively. Although the order of inhibition does not match, it falls within the experimental margin of error. More striking is the discrepancy in the (+)-huprines, since the

experimental values of IC_{50} show a great difference between (+)-HUY and the rest of the (+)-huprines.

Previous free energy calculations [16] performed using thermodynamic integration (TI) coupled to MD found free energy differences of -4.0 kcal·mol^{-1} from (-)-HUE to (-)-HUX, -3,8 kcal·mol^{-1} from (-)-HUM to (-)-HUY, -0.7 kcal·mol^{-1} from (-)-HUY to (-)-HUX, and -0,5 kcal·mol^{-1} from (-)-HUM to (-)-HUE. The greatest discrepancy between these data and our results is observed in the enhancement of the inhibitory potency by replacing the methyl group with an ethyl group in huprines (Table 2). This discrepancy can be associated with the fact that our results are based on quantum mechanical simulations, which allows the polarization of the ligand upon binding to be described.

More recent data for the inhibition of human recombinant AChE by both enantiomers of huprines X and Y are available in the literature.[21] Unfortunately, to the best of our knowledge there are no more recent data for the rest of the huprines studied here. A plot of the correlation between these last experimental data and our results is displayed in Figure 3 in order to verify the goodness of our results. Quantitative agreement between the theoretical and experimental binding free energy values is something difficult to achieve. However, as shown in Figure 3, the qualitative agreement of the order of the inhibition between theoretical and experimental values can be achieved by means of the alchemical FEP method. Previously, we found that this method was able to reproduce the experimental affinity order for several AChE inhibitors that exhibit quite different K_i values [22]. Now, we have verified that the alchemical FEP method is capable of reproducing the tendency on the inhibition power of a family of molecules with relatively close IC_{50} values. Therefore, this method represents a good compromise between computer resources and quality of results.

Analysis of the Geometric Parameters and Interaction Energy per Residue

To explain the different affinity of these huprines for AChE, an analysis of the geometric parameters and the interaction energy (IE) per residue between the ligand and the environment was performed. These parameters are reported as the average of the last 500 ps structures from the 1 ns AM1/MM MD simulation trajectories, once the system was

equilibrated. The potential energy evolution and RMSD evolution of the AChE backbone for the AChE-huprine systems as a function of the simulation time are reported in the supporting information (Figure S1).

(-)-Huprines

The main interactions between the residues of the gorge and huprine (-)-HUY are depicted in Figure 4, and selected geometrical parameters for (-)-huprines are reported in Table 3. As can be seen in Figure 4a, the polar residues of the gorge are connected between them and with the inhibitor by a network of hydrogen bonds mediated by a layer of water molecules. A similar network was previously observed for several classical AChE inhibitors [22] and also reported in the literature [40-43,19]. These water molecules reinforce the interactions between the residues of the gorge and the inhibitors, as the interaction between Asp72 and the primary amino group of (-)-huprines. This residue contributes significantly to the stabilization of the inhibitor at the active site of the enzyme (Figure 5), and its IE lowers from (-)-HUX to (-)-HUM. The distance between the carboxylate group of Asp72 and the hydrogen of the amino group of (-)-HUX is considerably shorter than in the other (-)-huprines.

Table 3 Selected averaged geometrical parameters for (-)-huprines (values of the distances are given in Å)

Distance (Å)	(-)-HUX	(-)-HUY	(-)-HUE	(-)-HUM
OD1(Asp72)-H12'$_1$ Huprine	3.86 ± 0.19	4.56 ± 0.30	4.86 ± 0.52	4.60 ± 0.26
O (His440) – H5 Huprine	1.98 ± 0.18	2.10 ± 0.18	1.96 ± 0.17	2.09 ± 0.19
OE1(Glu199) – H7 Huprine	2.49 ± 0.13	2.66 ± 0.16	2.67 ± 0.20	2.64 ± 0.18
OE2(Glu199) – N5 Huprine	5.99 ± 0.33	6.30 ± 0.24	5.61 ± 0.22	6.20 ± 0.35
OD1(Asp72) – N5 Huprine	8.04 ± 0.17	8.72 ± 0.21	9.04 ± 0.47	9.00 ± 0.26
CG(Phe 330) – C4 Huprine	3.54 ± 0.15	3.47 ± 0.14	4.01 ± 0.24	3.77 ± 0.21
CD2(Phe330) – N5 Huprine	3.94 ± 0.27	3.69 ± 0.21	4.39 ± 0.29	3.88 ± 0.25
CE2(Phe330) – C11a Huprine	4.07 ± 0.27	3.78 ± 0.20	4.28 ± 0.30	3.97 ± 0.24
CE2(Phe330) – C5a Huprine	4.17 ± 0.31	3.90 ± 0.22	4.79 ± 0.30	4.03 ± 0.27
CE1(Phe330) – C1 Huprine	3.49 ± 0.19	3.48 ± 0.20	3.48 ± 0.18	3.55 ± 0.20

CZ(Phe330) – C12 Huprine	3.71 ± 0.23	3.59 ± 0.18	3.90 ± 0.19	3.58 ± 0.18
CE1(Phe330) – C12a Huprine	3.65 ± 0.18	3.67 ± 0.18	4.04 ± 0.22	3.52 ± 0.19
CD1(Phe330) – C3 Huprine	3.42 ± 0.14	3.47 ± 0.14	3.98 ± 0.26	3.79 ± 0.21
CG(Trp84) – C12 Huprine	3.65 ± 0.17	3.78 ± 0.14	3.56 ± 0.14	3.87 ± 0.19
CE2 (Trp84) – N5 Huprine	3.94 ± 0.19	4.39 ± 0.29	3.85 ± 0.21	4.02 ± 0.20

Another key residue to stabilize inhibitors in the active site of the enzyme is His440. As previously reported in the crystal structure of the (-)-HUX-AChE complex [19], the aromatic nitrogen of the huprine is hydrogen-bonded with the main-chain carbonyl oxygen of His440. This interaction is conserved in all (-)-huprines (Figure 4a), and similar interaction energies of His440 in (-)-huprines-AChE systems are observed (Figure 5). IE values are slightly more favorable for (-)-huprines with an ethyl group in R_9, which correlates with shorter distances between the hydrogen of the aromatic nitrogen and the histidine oxygen.

Glu199 is the residue that most contributes to the interaction energy in most huprines (Figure 5), in agreement with previous studies [44]. Glu199 presents several interactions with the surrounding residues mediated by water molecules. It also presents nonclassical C-H···O hydrogen bonds, in particular with the hydrogen of one chiral carbon atom of the molecule, namely the bridgehead carbon atom at position 7. These interactions take place in the surroundings of the aromatic nitrogen of the huprines, and the IE of Glu199 is related to the distance between its carboxylic group and this nitrogen (Table 3 and Figure 5). A similar relationship is established between the IE of Asp72 and the distance of its carboxylic group to the aromatic nitrogen of (-)-huprines.

Due to the nature of the forces involved in the interaction between the ligand and the aromatic residues, the analysis of the interaction energy per residue is not evident in this case (Figure S3 of the supporting information). Therefore, an analysis was performed taking into account the contribution of these residues in an additive way. Huprines undergo parallel cation-π interactions with residues Trp84 and Phe330 (Figure 4b). We have added the IE of Trp84 and Phe330 (Figure 6a) to evaluate the effect that the substituents in R_3 and R_9 have in the modulation of the π–π stacking interactions. The (-)-huprine that has a better interaction is (-)-HUM, which features a methyl group in R_9 and a hydrogen atom in R_3. When a chlorine atom is added in R_3, the IE of the aromatic residues involved in the cation-π interaction

decrease. This can be explained by the fact that the relative position between Phe330 and the quinoline unit of (-)-HUY changed, bringing the benzyl group of the residue closer to the charged nitrogen of (-)-HUY. The distances CG(Phe330)–C4, CD2(Phe330)–N5, CE2(Phe330)–C11a, and CE2(Phe330)–C5a are shorter in (-)-HUY than in (-)-HUM, whereas the distance CE1(Phe330)–C12a is slightly longer in (-)-HUY (Table 3). Moreover, the relative position between Trp84 and the quinoline unit of (-)-HUY also changes, so that the distance CG(Trp84)–C12 decreases and the distance CE2(Trp84)–N5 increases. Substitution of methyl by ethyl at R_9, without the presence of chlorine at R_3 [(-)-HUE], also adversely affects the cation-π interaction. The presence of a bulkier group in R_9 displaces the quinoline unit of huprine relative to its position between Trp84 and Phe330, hindering their interaction (Table 3, Figure 6a). In this case, unlike in (-)-HUY, distances CG(Phe330)–C4, CD2(Phe330)–N5, CE2(Phe330)–C11a, and CE2(Phe330)–C5a increase. But in (-)-HUE the distances CZ(Phe330)–C12 and CE1(Phe330)–C12a also increase, indicating that both rings are distanced because of a steric hindrance due to the ethyl group. As a consequence the quinoline unit of (-)-HUE approaches Trp84 (Table 3). Surprisingly, by replacing the hydrogen of position R_3 with chlorine in (-)-HUE, thus converting it into (-)-HUX, the cation-π interaction improves. As in the previous case, the ethyl group in R_9 shifts the huprine from residue Phe330 to Trp84, but here another bulky group in R_3 restrains this movement. The distances discussed above for (-)-HUE follow the same trend in (-)-HUX but with smaller displacements. In addition, the distance CD1(Phe330)–C3 decreases with respect to the value that it had in (-)-HUM in those huprines having a chlorine atom in R_3, whereas it increases in (-)-HUE. All this suggests that the presence of bulkier substituents in R_3 or R_9 causes displacements in the relative position of huprines with respect to Phe330 and Trp84, disturbing the cation-π interaction. The simultaneous presence of bulky groups in both positions restricts these displacements and, in consequence, this interaction is impeded less. These displacements are also reflected in the interaction of the (-)-huprines with the catalytic triad (Figure 6b), a bulkier group in R_9 displaces the huprine toward His440 (see distances in Table 3), thereby improving this interaction. However, this is less pronounced when there is another bulky substituent in R_3. The IE profile is smoothed when the interactions due to the catalytic triad are added to the cation-π ones (Figure 6c).

The effect of a chlorine atom in R_3

According to the experimental data [16,14,21] and to the FEP results, (-)-huprines having a chlorine at position R_3 are the most potent inhibitors. However, the chlorine atom adversely affects the cation-π interaction, as seen above. It has been proposed that the contribution of the chlorine atom to the interaction between these inhibitors and the enzyme is due to nonspecific close spatial contacts with the hydrophobic pocket [19]. Therefore, the contribution of the residues surrounding the chlorine atoms to the IE should be larger in the systems with a chlorine atom in R_3 in relation to their counterparts with a hydrogen atom in this position. As depicted in Figure 4b and reported in Table S1 of the supporting information, the closest residues to the chlorine atoms are Phe330, Trp432, Met436, and Ile439. However, the greater contribution of Phe330 to this IE is due to the cation-π component. The total contributions of these residues to the IE, including and excluding Phe330, are reported in Figure S4 of the supporting information. Values that involve Phe330 do not represent solely the interaction with chlorine, and if we do not take into account the contribution of Phe330, the results are clearly unfavorable.

The pocket where the chlorine atom is accommodated includes a network of aromatic residues that are connected by π-stacking interactions and hydrogen bonds. Thus, Trp432 is hydrogen bonded to Tyr442, which is also hydrogen bonded to Trp84 (see Table S1 in the supporting information). Moreover, there is another tyrosine residue (Tyr334) interacting with Phe330 and hydrogen bonded to Asp72. In this way, Tyr334 and Tyr442 connect the residues that directly interact with the chlorine atom with those involved in the cation-π interaction and with Asp72. Therefore, the effect of this cluster of residues in the IE is analyzed in an additive way (Figure 7): first, by including the contribution of Tyr334 and Tyr442 to the interaction energy due to the residues that are closest to the chlorine atom (not including Phe330); later, by expanding this group with the contribution of Asp72 residue; and finally, by also introducing the effect of the residues involved in the cation-π interaction. By adding the effect of both tyrosine residues to the interaction energy of Trp432, Met436, and Ile 439, the total interaction energy of these residues is now negative. However, there is no proof that the contribution of the chlorine atom is due to close contacts, because the difference in IE in the systems with a chlorine atom in R_3 in relation to their counterparts with a hydrogen atom in the same position is less than 1 kcal·mol^{-1}. Adding the effect of Asp72 to the previous contribution shows that the difference in IE between (-)-HUX and (-)-HUE is around -8 kcal·mol^{-1}, and between (-)-HUY and (-)-HUM it is around -6 kcal·mol^{-1}. If we also add the effect of the residues involved in the cation-π interaction, these differences

become -9 and -0.36 kcal·mol^{-1}, respectively. These results suggest that the effect of chlorine atoms is more noticeable in a residue that is quite far away – at 8 Å (as Asp72) – than in the closest ones (Trp432, Met436, and Ile439). On the other hand, the contribution due to the cation-π interaction compensates this effect since the presence of a chlorine atom has an unfavorable effect on the interaction, especially in the huprines with a methyl group in R_9.

The effect of ethyl group in R_9

The ethyl group in R_9 fills a hydrophobic pocket formed by Tyr121, Phe290, Phe330, and Phe331. The total contribution of these residues to the IE fails to explain the greater affinity of the (-)-huprines having an ethyl group in R_9 with respect to the huprines having a methyl group in this position (Figure 8). However, we should keep in mind that the greater contribution of Phe330 to the IE is due to the cation-π interaction, and an ethyl group in R_9 does not favor this interaction. By removing the contribution of Phe330 in this IE, contradictory results are obtained for compounds with chlorine and those without chlorine. The methyl/ethyl group in R_9 is close to the residues of the oxyanion hole (Gly118, Gly119), but the effect that these latter residues have on the IE is not significant. Nevertheless, residues of the hydrophobic pocket form a network of interactions with Phe288, Ser122, His440, Ser200, and Glu199. The IE obtained by adding the contribution of these residues is consistent with the higher affinity of the enzyme for inhibitors having an ethyl group at R_9 relative to those having a methyl group. Finally, residues forming the cation-π interaction (Phe330 and Trp84) do not modify this tendency. Thus, it seems that the effect of the ethyl group in position R_9 cannot be explained by short-range interactions, but as in the case of the chlorine atom in R_3, it is due to a network of interactions in the gorge. In these networks aromatic residues, as well as polar residues, and several water molecules are involved. This is consistent with the binding free energy results obtained by means of the alchemical FEP method, where the contribution of the van der Waals term was almost as important as the electrostatic term.

(+)-Huprines

The arrangement of (+)-huprines in the gorge differs from that of the (-)-huprines (Figure 9): the primary amino group of (+)-huprines interacts with the backbone oxygen of His440, and the protonated aromatic nitrogen of the inhibitor is interacting with Ser122 through a water molecule. (+)-Huprines also undergo parallel cation-π interactions with

residues Trp84 and Phe330. However, Asp72 does not interact with the amino group of (+)-huprines, since this group is located on the other side of the molecule with respect to the residue. In the (+)-HUE-AChE complex, Asp72 interacts with two water molecules, with Tyr334 and with H3 of the inhibitor (Figure 9). The interactions with tyrosine and water molecules are retained in the other (+)-huprine systems, although the distances with the water molecules are longer, especially in the case of huprines with a chlorine atom in R_3. This is evident in the case of (+)-HUX, where the presence of chlorine disrupts these interactions and there is only one water molecule in this position. In the latter case, the lowest value of the Asp72 interaction energy is obtained (Figure 5). The amino group of (+)-huprines interacts with the carbonyl oxygen of His440. Nevertheless, these distances are longer than the distances between (-)-huprine aromatic nitrogen and histidine oxygen, which is reflected in the values of IE for His440 (Figure 5). The presence of an ethyl group at R_9 favors this interaction, as seen in the IE. In the (+)-HUX-AChE system, the repulsion between the chlorine and Asp72 pushes away the inhibitor toward the histidine 440, which leads to a shorter distance between the amino group of the inhibitor and the histidine and, hence, to a more favorable IE. The geometrical parameters in the relationship between residue Asp72, residue Glu199, and the N^+ atom of the ligand are reported in Figure S2 of the supporting information. The longer distance between Asp72 and the aromatic nitrogen of the inhibitor in the (+)-HUX-AChE system relative to other (+)-huprine-AChE complexes evidences this displacement. Glu199 forms non-classical C-H···O hydrogen bonds with hydrogen atoms of the carbobicyclic ring of the huprines and this residue also forms a hydrogen bond with Tyr130. Moreover, both residues are involved in a network of water-mediated hydrogen bonds with other residues and the inhibitor (Figure 9a). However, the relationship between the Glu199 IE and the geometrical parameters is not evident for (+)-huprines. Paradoxically, the contribution of Ser122 to the IE is relatively small even though this residue is forming a hydrogen bond mediated by a water molecule with the charged aromatic nitrogen.

BIEs

Binding isotope effects for inhibitors isotopically labeled with ^{13}C, ^{15}N, and ^{18}O atoms were computed in this work using the QM/MM method based on 11 optimized structures of inhibitors dissolved in water and bound in the active site of AChE. As stated above, these structures were selected each 20 ps from the last 200 ps of the long QM/MM MD simulations.

A BIE value equal to 1 means that no binding isotope effect is observed. The average values <1 indicate an inverse BIE, which means that the isotopically substituted atom has a stronger interaction in the enzyme than in water. The average values >1 indicate a direct BIE [30, 39]. It is important to note that average values of BIEs other than 1 were expected only in the case of important electrostatic enzyme-ligand interactions being present in the gorge.

In (-)-huprine-AChE systems no significant BIEs are observed. This is consistent with our previous study, where no significant BIEs for tacrine or huperzine A were observed [22]. Since (-)-huprines are tacrine-huperzine hybrids that retain the most significant interactions with AChE, no significant BIEs are expected. In the (+)-huprines-AChE systems most substitutions lead to non-representative BIEs. However, small direct BIEs, namely 1.011 ± 0.002 and 1.011 ± 0.003, are detected in the nitrogen of the amino group of (+)-HUE and (+)-HUX, respectively. This result indicates that the hydrogen bonds established between the amino group of these huprines and the water molecules of the solvent are more favorable than the interactions with the enzyme, despite the low value of the BIE.

AChE is a singular enzyme, whose active site is a deep cavity of 20 Å composed of several aromatic residues interacting between them and with the inhibitors by π-stacking interactions. This cleft is full of water molecules that enable a network of hydrogen bond interactions between the polar residues of the gorge and the inhibitor. Moreover, due to their hydroxyl group, some tyrosine residues act as bridges that connect the bulk of aromatic and polar residues of AChE. All these particularities result in the singular interactions between the enzyme and the inhibitors. The nature of the hydrophobic interactions and the similar intensity of the hydrophilic interactions in water and enzyme do not lead to any remarkable BIEs.

Conclusions

The alchemical free energy perturbation method, based on MD simulations within hybrid QM/MM potentials, has been used to calculate the binding free energy of a set of huprines with AChE. Previously, it was verified that this method was appropriate to distinguish AChE ligands that present large differences in inhibitory activity at a reasonable computational cost [22]. (-)-Huprines have been found to be more effective inhibitors than

their corresponding enantiomers, in agreement with the experimental results. Present results reproduce the experimental inhibitory tendency [21] for both huprine X and huprine Y enantiomers. The present study points to this method as a suitable approach to distinguish between inhibitors of similar potencies. Findings also reveal the importance of the van der Waals interaction in the inhibition process since the contribution of this term is almost as important as the electrostatic one. The analysis of the geometrical parameters and interaction energy per residue confirm these data and highlight the nature of this singular enzyme. BIE results also corroborate the distinctive features of AChE, since no significant BIEs were observed in systems with some important electrostatic interactions. This can be attributed to the large number of water molecules involved in the interactions between the inhibitors and the enzyme.

Asp72, Glu199, and His440 are the residues that contribute most to the interaction energy with the inhibitors. The amino group of (-)-huprines interacts with Asp72 through one or two water molecules, whereas the aromatic nitrogen forms a direct hydrogen bond with the carbonyl oxygen of His440. These residues stretch the inhibitor in opposite directions and the balance of forces is conditioned by the substituents at R_3 and R_9. A bulky group at R_9 (ethyl) displaces the inhibitors toward His440, thereby promoting this interaction, albeit at the expense of disturbing the cation-π interaction with Phe330 and Trp84. The steric hindrance due to the ethyl group causes the quinoline unit of huprine to move away form residue Phe330 and to approach residue Trp84. On the contrary, if there is a chlorine atom at R_3 the His440 interaction energy decreases. In this case the sandwich-π interaction with Phe330 and Trp84 is also affected because the relative position between the quinoline unit of (-)-HUY and these residues changes. The simultaneous presence of bulky groups at R_3 and R_9 leads to more restrained displacements and less affected cation-π interaction. The high contribution of Glu199 to the IE seems difficult to explain based on its non-classical C-H···O hydrogen bond with the inhibitor. However, it is involved in a hydrogen bond network mediated by water molecules with residues of the catalytic triad in the vicinity of the charged aromatic nitrogen of (-)-huprines.

The effect that a chlorine atom at the R_3 position has on the inhibitory efficiency cannot be explained by means of the contribution of the surrounding residues to the interaction energy. The same observation is valid for the effect of the ethyl group at R_9. Thus, stabilization due to short-range interactions can be ruled out. Actually, it seems that a

cooperative effect of the residues of the gorge determines the affinity of the enzyme for these inhibitors. Asp72, Glu199, and His440 contribute significantly to the network of interactions between active site residues, which stabilize the inhibitors in the gorge.

(+)-Huprines are the less active enantiomers, whose arrangement in the active site differs in some aspects from that of (-)-huprines. However, Asp72, Glu199, and His440 are also the residues that contribute most to the IE, even though the relationship between these IE tendencies and the geometrical parameters is not always evident. Emphasis is given to the low contribution of Ser122 to the IE, although this residue forms a hydrogen bond with the aromatic nitrogen of (+)-huprines mediated by a water molecule. This also indicates that the affinity for the inhibitor is due to a cooperative effect of the whole enzyme, where Asp72, Glu199, and His440 make a prominent contribution.

Electronic supplementary information

RMSD plots. Geometrical parameters in the relationship between residue Asp72, residue Glu199, and N^+ atom of the ligand. Selected IE of some residues in the huprine-AChE systems. Selected averaged distances involving the chlorine atom and the surrounding residues for (-)-HUX and (-)-HUY systems.

Conflicts of interest

There are no conflicts of interest to declare.

Figure Captions

Fig. 1 Binding free energy in kcal·mol^{-1}. The contribution of electrostatic and van der Waals terms are depicted in red and blue, respectively. The percentage of these contributions to the total energy is also indicated

Fig. 2 Correlation between experimental [16,14] and calculated values of binding free energy

Fig. 3 Correlation between experimental [21] and calculated values of binding free energy

Fig. 4 Plots of the main interactions between (-)-HUY and the subset of residues forming the binding pocket. Some selected average distances in Å are depicted

Fig. 5 Average IE of polar residues in the AChE-huprine systems (all values are given in kcal·mol^{-1})

Fig. 6 Average values of the sum of interaction energies (in kcal·mol^{-1}) of (a) aromatic residues involved in the cation-π interaction, (b) residues of the catalytic triad and, (c) residues of the catalytic triad plus aromatic residues involved in the cation-π interaction

Fig. 7 Average values of the addition of interaction energies (in kcal·mol^{-1}) of (a) Trp432 + Met436 + Ile 439+ Tyr442 + Tyr334, (b) Asp72 + Trp432 + Met436 + Ile 439+ Tyr442 + Tyr334, and (c) Asp72 + Trp84 + Phe 330 + Trp432 + Met436 + Ile 439+ Tyr442 + Tyr334, in the (-)-huprine-AChE systems

Fig. 8 Average values of the addition of interaction energies (in kcal·mol^{-1}) of (a) Tyr121 + Phe290 + Phe330 + Phe331, (b) Tyr121 + Phe290 + Phe331, (c) Gly118 + Gly119+ Ser122 + Tyr121 + Glu199 + Ser200 + Phe288 + Phe290 + Phe331 + His440, and (d) Trp84 + Gly118 + Gly119+ Ser122 + Tyr121 + Glu199 + Ser200 + Phe288 + Phe290 + Phe330 + Phe331 + His440, in the (-)-huprine-AChE systems

Fig. 9 Plot of the main interactions between (+)-HUE and the subset of residues forming the binding pocket. Some selected average distances in Å are depicted

References

1. Bossy-Wetzel E, Schwarzenbacher R, Lipton SA (2004) Molecular Pathways to Neurodegeneration. Nat Med 10 (7):S2-S9
2. Bartus R, Dean R, Beer B, Lippa A (1982) The Cholinergic Hypothesis of Geriatric Memory Dysfunction. Science 217 (4558):408-414
3. Dunnett SB, Fibiger HC (1993) Role of Forebrain Cholinergic Systems in Learning and Memory - Relevance to the Cognitive Deficits of Aging and Alzheimer Dementia. In: Cuello AC (ed) Cholinergic Function and Dysfunction, vol 98. Progress in Brain Research. Elsevier Science Publ B V, Amsterdam, pp 413-420
4. Weinstock M (1997) Possible Role of the Cholinergic System and Disease Models. J of Neural Transm-Suppl (49):93-102
5. Rang HP, Dale MM, Ritter JM, Flower RJ, Henderson G (2012) Rang & Dale's Pharmacology. 7th edn. Elsevier
6. Bar-On P, Millard CB, Harel M, Dvir H, Enz A, Sussman JL, Silman I (2002) Kinetic and Structural Studies on the Interaction of Cholinesterases with the Anti-Alzheimer Drug Rivastigmine. Biochemistry 41 (11):3555-3564
7. Harel M, Schalk I, Ehretsabatier L, Bouet F, Goeldner M, Hirth C, Axelsen PH, Silman I, Sussman JL (1993) Quaternary Ligand-Binding to Aromatic Residues in the Active-Site Gorge of Acetylcholinesterase. Proc Natl Acad Sci U S A 90 (19):9031–9035
8. Kryger G, Silman I, Sussman JL (1999) Structure of Acetylcholinesterase Complexed with E2020 (Aricept (R)): Implications for the Design of New Anti-Alzheimer Drugs. Structure 7 (3):297-307
9. Greenblatt HM, Kryger G, Lewis T, Silman I, Sussman JL (1999) Structure of Acetylcholinesterase Complexed with (-)-galantamine at 2.3 Angstrom Resolution. FEBS Lett 463 (3):321-326
10. Gilson MK, Zhou HX (2007) Calculation of Protein-Ligand Binding Affinities. In: Annual Review of Biophysics and Biomolecular Structure, vol 36. Annual Review of Biophysics. Annual Reviews, Palo Alto, pp 21-42.
11. Sham YY, Chu ZT, Tao H, Warshel A (2000) Examining Methods for Calculations of Binding Free Energies: LRA, LIE, PDLD-LRA, and PDLD/S-LRA Calculations of Ligands Binding to an HIV protease. Proteins-Struct Funct and Genet 39 (4):393-407
12. Hansen N, van Gunsteren WF (2014) Practical Aspects of Free-Energy Calculations: A Review. J Chem Theory Comput 10 (7):2632-2647
13. Wlodek ST, Antosiewicz J, McCammon JA, Straatsma TP, Gilson MK, Briggs JM (1996) Binding of Tacrine and 6-Chlorotacrine by Acetylcholinesterase. Biopolymers 38 (1):109-117
14. Camps P, El Achab R, Görbig DM, Morral J, Muñoz-Torrero D, Badia A, Baños JE, Vivas NM, Barril X, Orozco M, Luque FJ (1999) Synthesis, in Vitro Pharmacology, and Molecular Modelling of Very Potent Tacrine-Huperzine A Hybrids as Acetylcholinesterase Inhibitors of Potential Interest for the Treatment of Alzheimer's Disease. J Med Chem 42:3227-3242
15. Barril X, Orozco M, Luque FJ (1999) Predicting Relative Binding Free Energies of Tacrine-Huperzine A Hybrids as Inhibitors of Acetylcholinesterase. J Med Chem 42 (25):5110-5119
16. Camps P, El Achab R, Morral J, Muñoz-Torrero D, Badia A, Baños JE, Vivas NM, Barril X, Orozco M, Luque FJ (2000) New Tacrine-Huperzine A Hybrids (Huprines):

Highly Potent Tight-Binding Acetylcholinesterase Inhibitors of Interest for the Treatment of Alzheimer's Disease. J Med Chem 43 (24):4657-4666
17. Camps P, Gomez E, Muñoz-Torrero D, Badia A, Vivas NM, Barril X, Orozco M, Luque FJ (2001) Synthesis, in Vitro Pharmacology, and Molecular Modeling of Syn-Huprines as Acetylcholinesterase Inhibitors. J Med Chem 44 (26):4733-4736
18. Barril X, Gelpi JL, Lopez JM, Orozco M, Luque FJ (2001) How Accurate can Molecular Dynamics/Linear Response and Poisson-Boltzmann/Solvent Accessible Surface Calculations be for Predicting Relative Binding Affinities? Acetylcholinesterase Huprine Inhibitors as a Test Case. Theor Chem Acc 106 (1-2):2-9
19. Dvir H, Wong DM, Harel M, Barril X, Orozco M, Luque FJ, Muñoz-Torrero D, Camps P, Rosenberry TL, Silman I, Sussman JL (2002) 3D Structure of *Torpedo californica* Acetylcholinesterase Complexed with Huprine X at 2.1 Å Resolution: Kinetic and Molecular Dynamic Correlates. Biochemistry 41 (9):2970-2981
20. Camps P, Gomez E, Muñoz-Torrero D, Badia A, Clos MV, Curutchet C, Muñoz-Muriedas J, Luque FJ (2006) Binding of 13-Amidohuprines to Acetylcholinesterase: Exploring the Ligand-Induced Conformational Change of the Gly117-Gly118 Peptide Bond in the Oxyanion Hole. J Med Chem 49 (23):6833-6840
21. Viayna E, Gomez T, Galdeano C, Ramirez L, Ratia M, Badia A, Clos MV, Verdaguer E, Junyent F, Camins A, Pallas M, Bartolini M, Mancini F, Andrisano V, Arce MP, Rodriguez-Franco MI, Bidon-Chanal A, Luque FJ, Camps P, Muñoz-Torrero D (2010) Novel Huprine Derivatives with Inhibitory Activity toward beta-Amyloid Aggregation and Formation as Disease-Modifying Anti-Alzheimer Drug Candidates. ChemMedChem 5 (11):1855-1870
22. Nascimento ECM, Oliva M, Swiderek K, Martins JBL, Andrés J (2017) Binding Analysis of Some Classical Acetylcholinesterase Inhibitors: Insights for a Rational Design Using Free Energy Perturbation Method Calculations with QM/MM MD Simulations. J Chem Inf Model 57:958-976
23. Camps P, Cusack B, Mallender WD, Achab RE, Morral J, Muñoz-Torrero D, Rosenberry TL (2000) Huprine X is a Novel High-Affinity Inhibitor of Acetylcholinesterase That Is of Interest for Treatment of Alzheimer's Disease. Mol Pharmacol 57 (2):409-417
24. Muñoz-Torrero D, Camps P (2008) Huprines for Alzheimer's Disease Drug Development. Expert Opin Drug Discov 3 (1):65-81
25. Roman S, Vivas NM, Badia A, Clos MV (2002) Interaction of a New Potent Anticholinesterasic Compound (+/-)Huprine X with Muscarinic Receptors in Rat Brain. Neurosci Lett 325 (2):103-106
26. Roman S, Badia A, Camps P, Clos MV (2004) Potentiation Effects of (+/-)Huprine X, a New Acetylcholinesterase Inhibitor, on Nicotinic Receptors in Rat Cortical Synaptosomes. Neuropharmacology 46 (1):95-102
27. Ratia M, Gimenez-Llort L, Camps P, Muñoz-Torrero D, Perez B, Clos MV, Badia A (2013) Huprine X and Huperzine A Improve Cognition and Regulate Some Neurochemical Processes Related with Alzheimer's Disease in Triple Transgenic Mice (3xTg-AD). Neurodegener Dis 11 (3):129-140
28. Shirts MR, Mobley DL, Chodera JD (2007) Alchemical Free Energy Calculations: Ready for Prime Time? Annu Rep Comput Chem 3:41-59
29. Wang L, Wu Y, Deng Y, Kim B, Pierce L, Krilov G, Lupyan D, Robinson S, Dahlgren MK, Greenwood J, Romero DL, Masse C, Knight JL, Steinbrecher T, Beuming T, Damm W, Harder E, Sherman W, Brewer M, Wester R, Murcko M, Frye L, Farid R, Lin T, Mobley DL, Jorgensen WL, Berne BJ, Friesner RA, Abel R (2015) Accurate and Reliable Prediction of Relative Ligand Binding Potency in Prospective Drug Discovery

by Way of a Modern Free-Energy Calculation Protocol and Force Field. J Am Chem Soc 137 (7):2695-2703
30. Schramm VL (2007) Binding Isotope Effects: Boon and Bane. Curr Opin Chem Biol 11 (5):529-536
31. Holm L, Park J (2000) DaliLite Workbench for Protein Structure Comparison. Bioinformatics 16 (6):566-567
32. Morris GM, Huey R, Lindstrom W, Sanner MF, Belew RK, Goodsell DS, Olson AJ (2009) AutoDock4 and AutoDockTools4: Automated Docking with Selective Receptor Flexibility. J Comput Chem 30 (16):2785-2791
33. Field MJ (1999) A Pratical Introduction to the Simulation of Molecular Systems. Cambridge University Press, Cambridge
34. Field MJ, Albe M, Bret C, Proust-de Martin F, Thomas A (2000) The Dynamo Library for Molecular Simulations Using Hybrid Quantum Mechanical and Molecular Mechanical Potentials. J Comput Chem 21 (12):1088-1100
35. Dewar MJS, Zoebisch EG, Healy EF, Stewart JJP (1985) Development and use of Quantum Mechanical Molecular Models. 76. AM1: A New General Purpose Quantum Mechanical Molecular Model. J Am Chem Soc 107 (13):3902-3909
36. Jorgensen WL, Maxwell DS, Tirado-Rives J (1996) Development and Testing of the OPLS All-Atom Force Field on Conformational Energetics and Properties of Organic Liquids. J Am Chem Soc 118 (45):11225-11236
37. Jorgensen WL, Chandrasekhar J, Madura JD, Impey RW, Klein ML (1983) Comparison of Simple Potential Functions for Simulating Liquid Water. J Chem Phys 79 (2):926-935
38. Świderek K, Martí S, Moliner V (2012) Theoretical Studies of HIV-1 Reverse Transcriptase Inhibition. Phys Chem Chem Phys 14 (36):12614-12624
39. Krzemińska A, Paneth P, Moliner V, Świderek K (2015) Binding Isotope Effects as a Tool for Distinguishing Hydrophobic and Hydrophilic Binding Sites of HIV-1 RT. J Phys Chem B 119 (3):917-927
40. Koellner G, Kryger G, Millard CB, Silman I, Sussman JL, Steiner T (2000) Active-Site Gorge and Buried Water Molecules in Crystal Structures of Acetylcholinesterase from Torpedo californica. J Mol Biol 296 (2):713-735
41. Henchman RH, McCammon JA (2002) Structural and dynamic properties of water around acetylcholinesterase. Protein Sci 11 (9):2080-2090
42. Henchman RH, Tai KS, Shen TY, McCammon JA (2002) Properties of Water Molecules in the Active Site Gorge of Acetylcholinesterase from Computer Simulation. Biophys J 82 (5):2671–2682
43. Ramos ASF, Techert S (2005) Influence of the Water Structure on the Acetylcholinesterase Efficiency. Biophys J 89 (3):1990-2003
44. Martín-Santamaría S, Muñoz-Muriedas J, Luque FJ, Gago F (2004) Modulation of Binding Strength in Several Classes of Active Site Inhibitors of Acetylcholinesterase Studied by Comparative Binding Energy Analysis. J Med Chem 47 (18):4471-4482

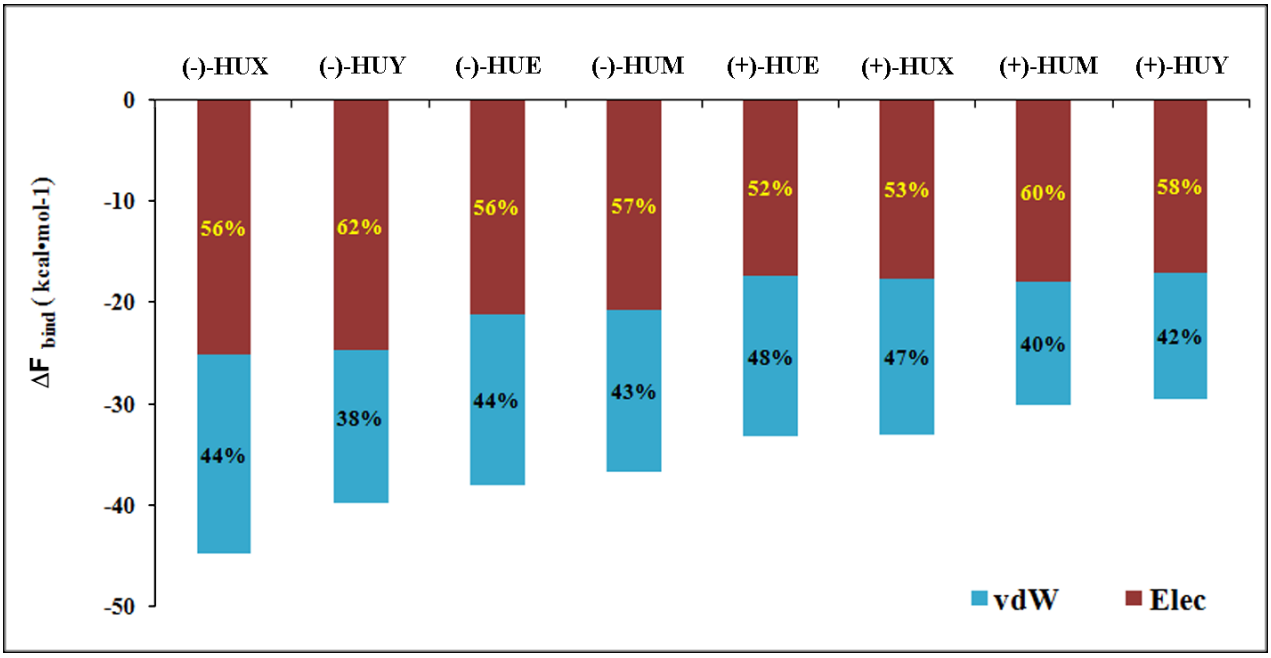
(-)-HUX
(-)-HUY
(-)-HUE
(-)-HUM
(+)-HUE
(+)-HUX
(+)-HUM
(+)-HUY
0
-10
-20
-30
-40
-50
ΔF bind (kcal•mol-1)
56%
62%
56%
57%
52%
53%
60%
58%
44%
38%
44%
43%
48%
47%
40%
42%
vdW
Elec

Figure 1

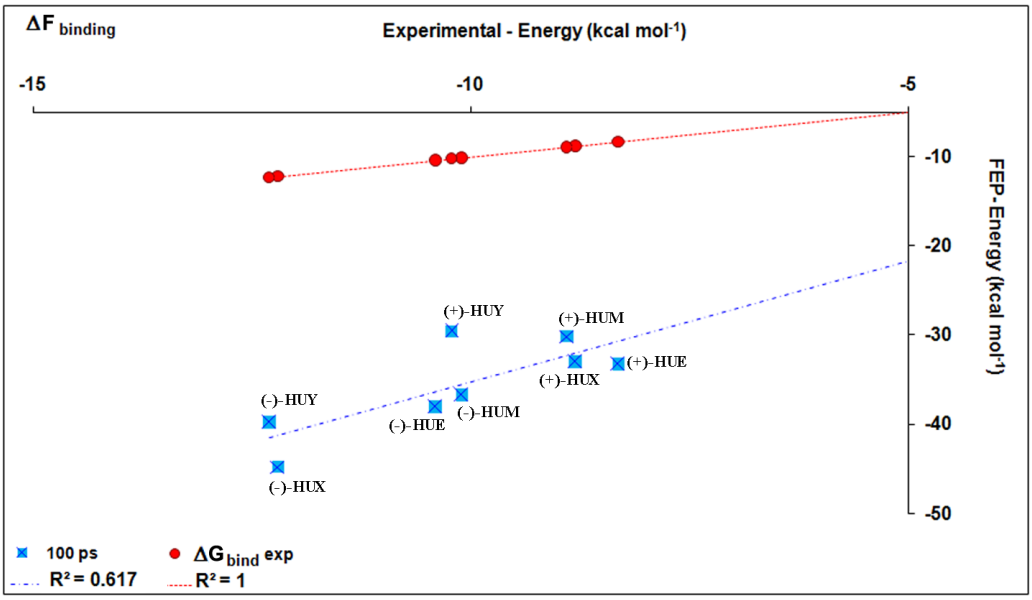
ΔF binding
Experimental - Energy (kcal mol-1)
-15
-10
-5
-10
-20
-30
-40
-50
FEP-Energy (kcal mol-1)
(+)-HUY
(+)-HUM
(+)-HUE
(+)-HUX
(-)-HUY
(-)-HUE
(-)-HUM
(-)-HUX
100 ps
ΔGbind exp
R² = 0.617
R² = 1

Figure 2

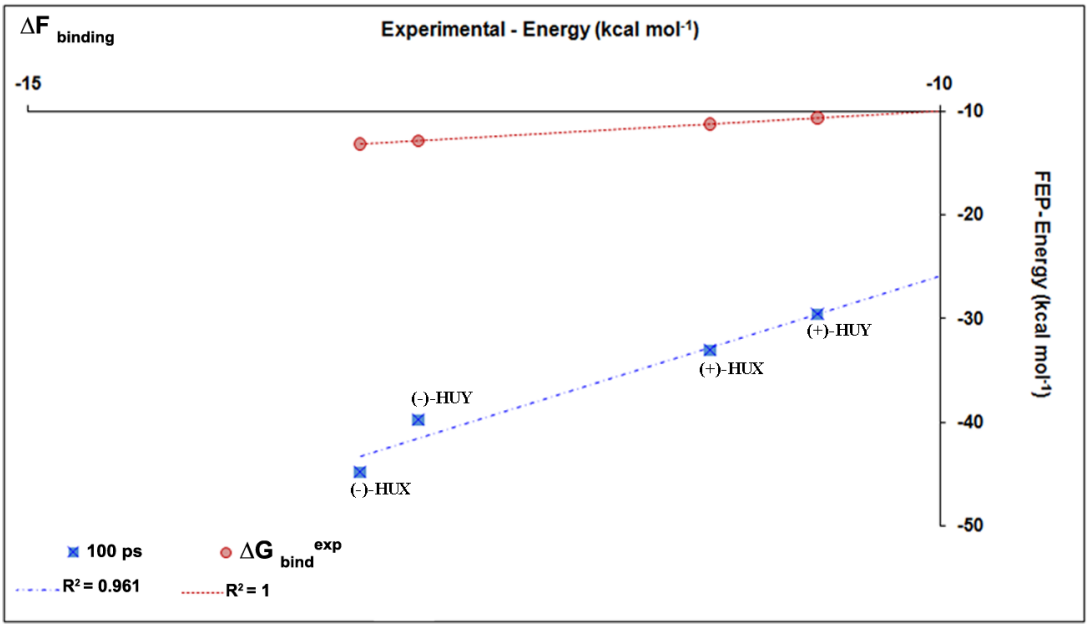
ΔF binding
Experimental - Energy (kcal mol-1)
-15
-10
-10
-20
-30
-40
-50
FEP-Energy (kcal mol-1)
(+)-HUY
(+)-HUX
(-)-HUY
(-)-HUX
100 ps
ΔG bind exp
R² = 0.961
R² = 1

Figure 3

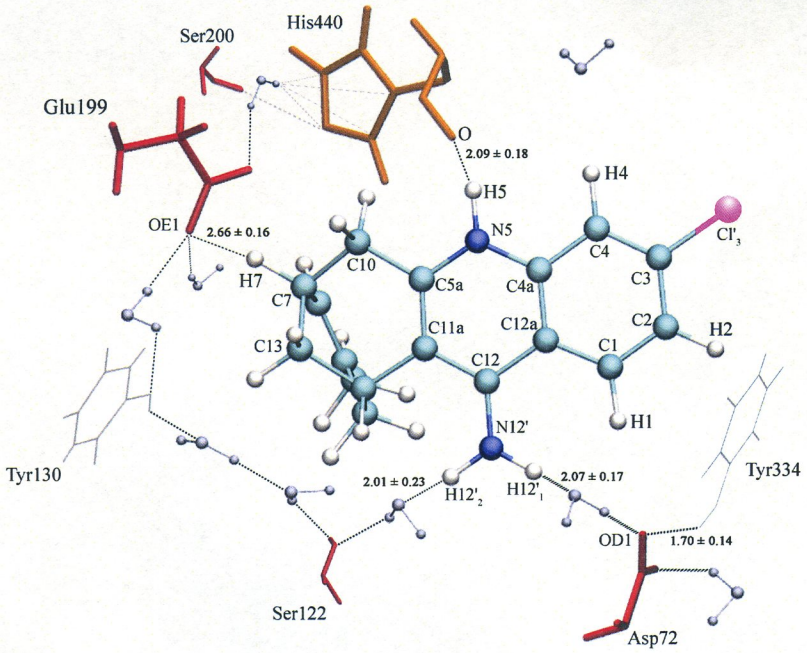
Ser200
His440
Glu199
O
2.09 ± 0.18
H5
H4
OE1
2.66 ± 0.16
N5
Cl'3
C4
C10
C5a
C4a
C3
H7
C7
C11a
C12a
C2
H2
C13
C12
C1
N12'
H1
Tyr130
2.01 ± 0.23
H12'2
H12'1
2.07 ± 0.17
Tyr334
OD1
1.70 ± 0.14
Ser122
Asp72

(a)

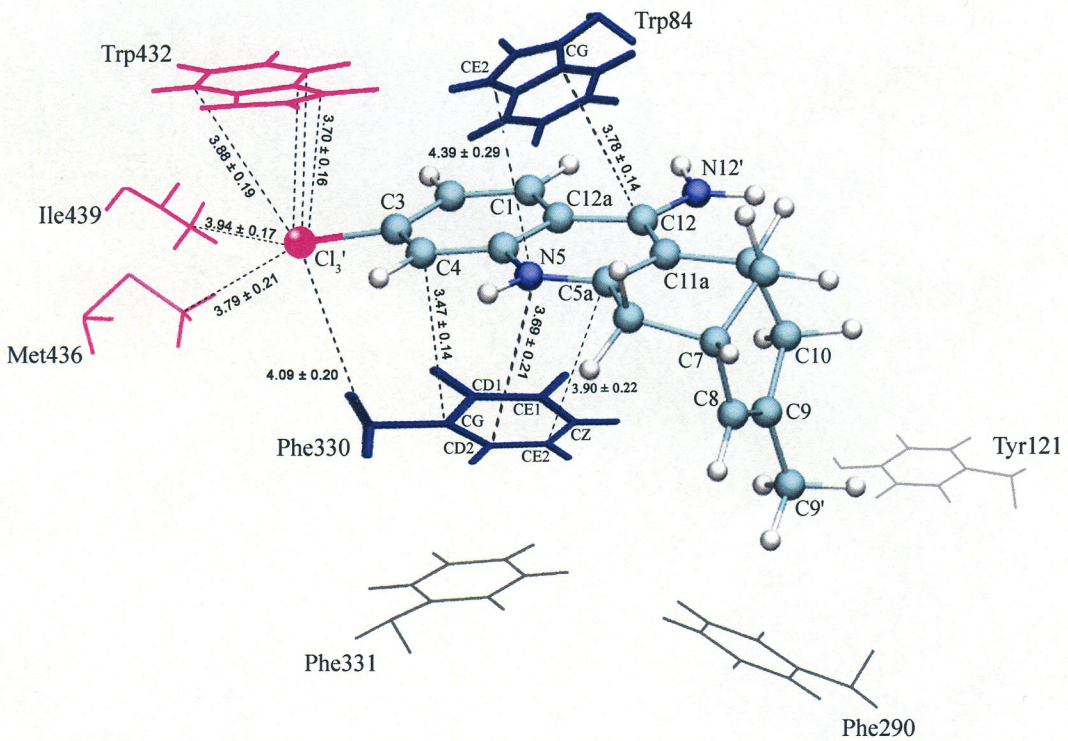
Trp84
Trp432
CE2
CG
3.88 ± 0.19
3.70 ± 0.16
4.39 ± 0.29
3.78 ± 0.14
N12'
C3
C1'
C12a
Ile439
3.94 ± 0.17
C12
Cl3'
C4
N5
C11a
3.79 ± 0.21
C5a
3.47 ± 0.14
3.69 ± 0.21
Met436
C7
C10
4.09 ± 0.20
CD1
3.90 ± 0.22
C8
CE1
C9
CG
CZ
Phe330
CD2
CE2
Tyr121
C9'
Phe331
Phe290

(b)

Figure 4

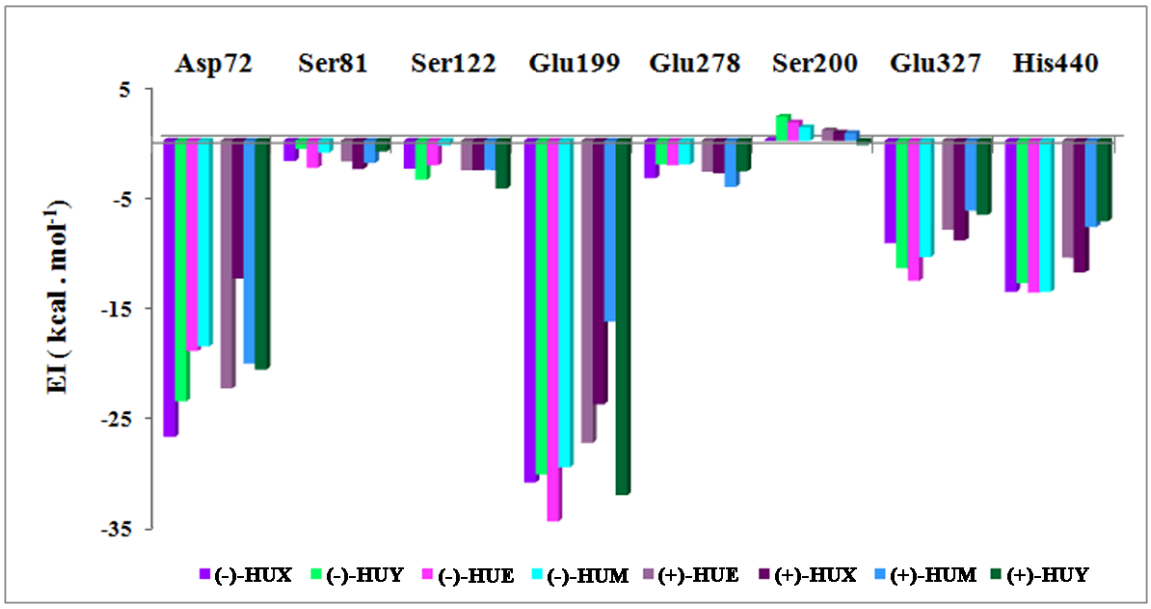
Asp72
Ser81
Ser122
Glu199
Glu278
Ser200
Glu327
His440
5
-5
-15
-25
-35
EI (kcal . mol-1)
(-)-HUX
(-)-HUY
(-)-HUE
(-)-HUM
(+)-HUE
(+)-HUX
(+)-HUM
(+)-HUY

Figure 5

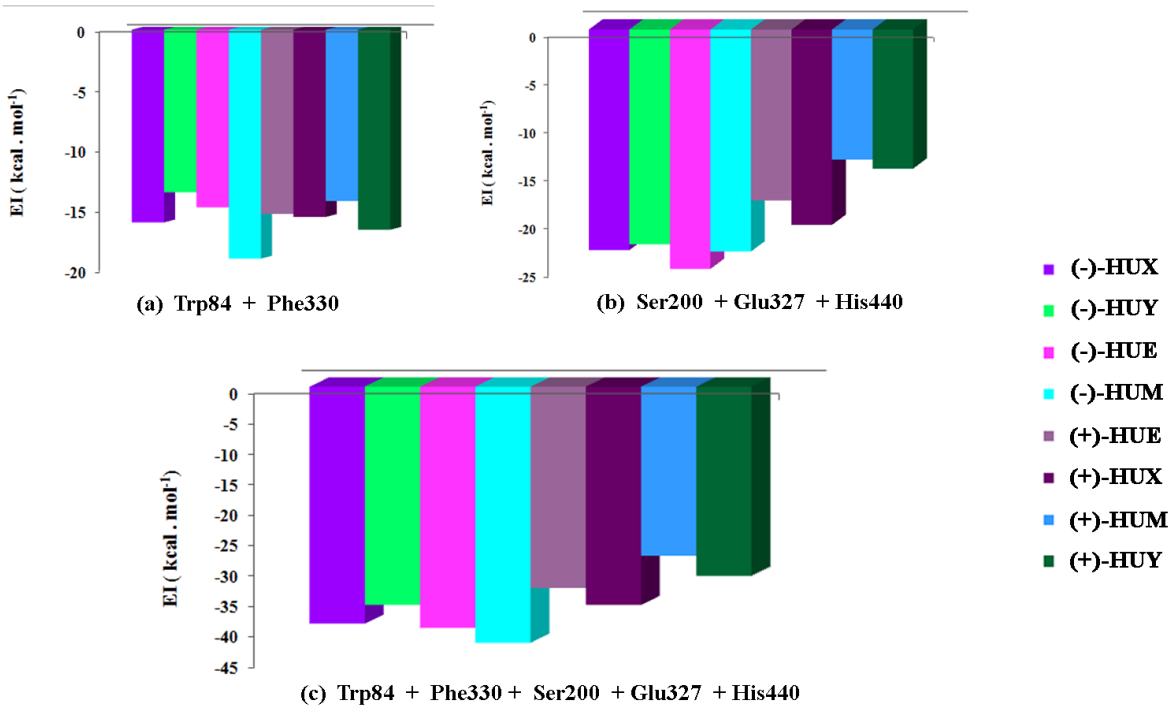
EI (kcal . mol-1)
0
-5
-10
-15
-20
(a) Trp84 + Phe330
-25
(b) Ser200 + Glu327 + His440
-30
-35
-40
-45
(c) Trp84 + Phe330 + Ser200 + Glu327 + His440
(-)-HUX
(-)-HUY
(-)-HUE
(-)-HUM
(+)-HUE
(+)-HUX
(+)-HUM
(+)-HUY

Figure 6

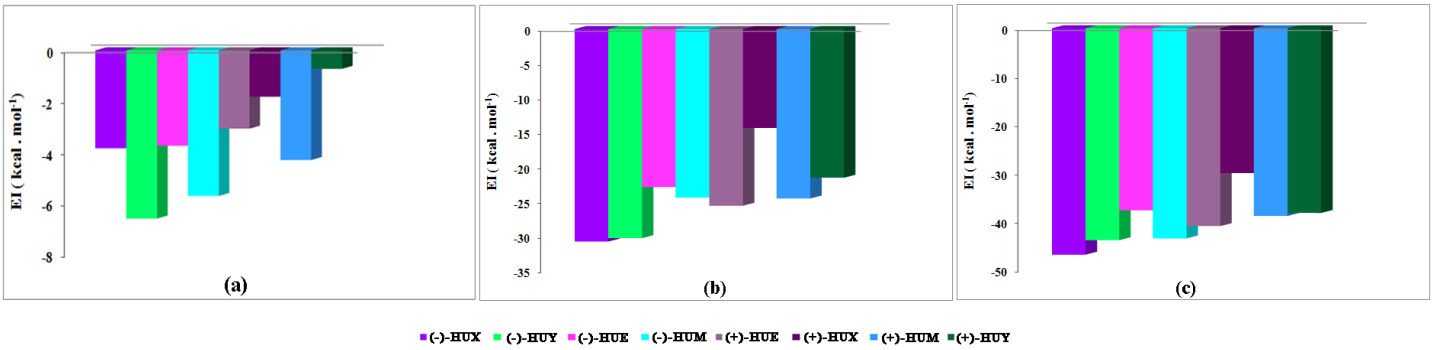
EI (kcal . mol-1)
0
-2
-4
-6
-8
(a)
EI (kcal . mol-1)
0
-5
-10
-15
-20
-25
-30
-35
(b)
EI (kcal . mol-1)
0
-10
-20
-30
-40
-50
(c)
(-)-HUX
(-)-HUY
(-)-HUE
(-)-HUM
(+)-HUE
(+)-HUX
(+)-HUM
(+)-HUY

Figure 7

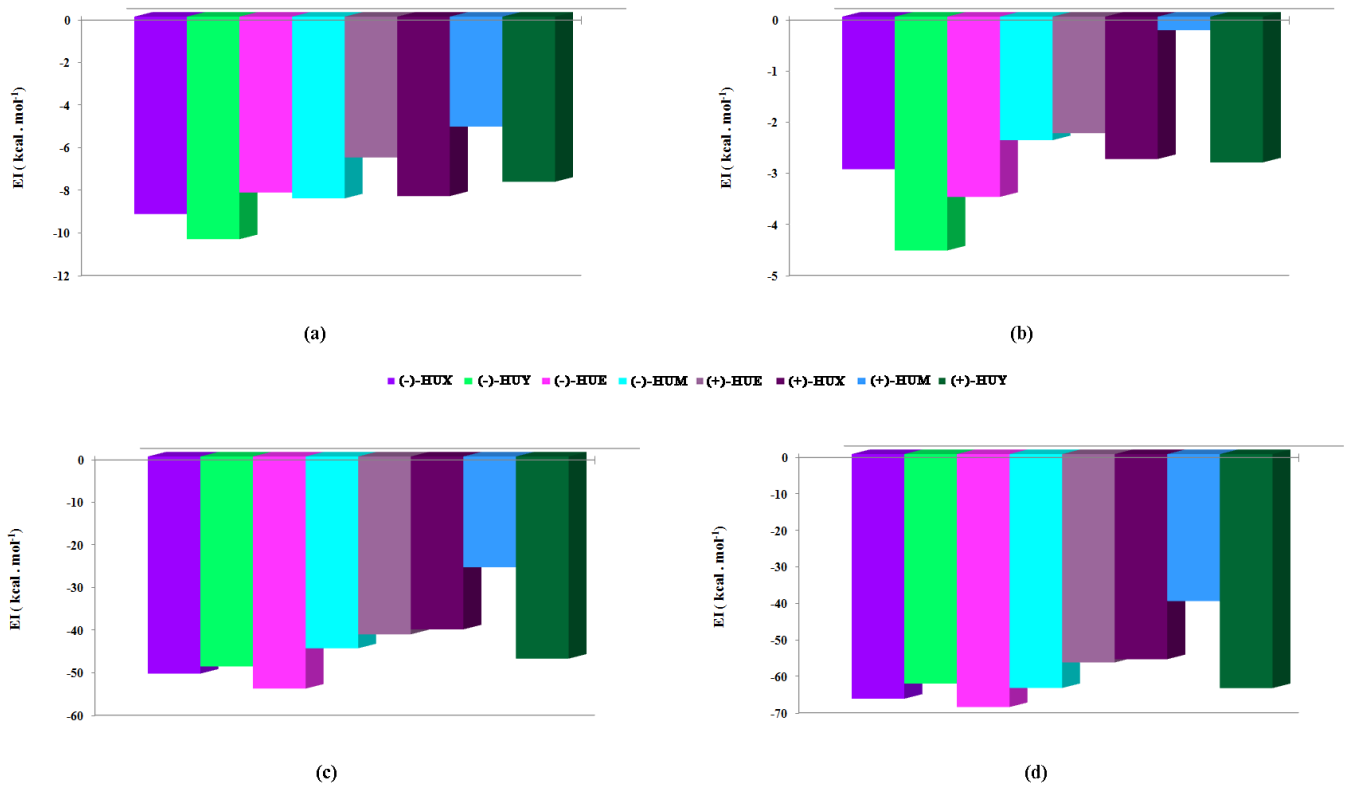
EI (kcal . mol-1)
0
-2
-4
-6
-8
-10
-12
(a)
EI (kcal . mol-1)
0
-1
-2
-3
-4
-5
(b)
(-)-HUX
(-)-HUY
(-)-HUE
(-)-HUM
(+)-HUE
(+)-HUX
(+)-HUM
(+)-HUY
EI (kcal . mol-1)
0
-10
-20
-30
-40
-50
-60
(c)
EI (kcal . mol-1)
0
-10
-20
-30
-40
-50
-60
-70
(d)

Figure 8

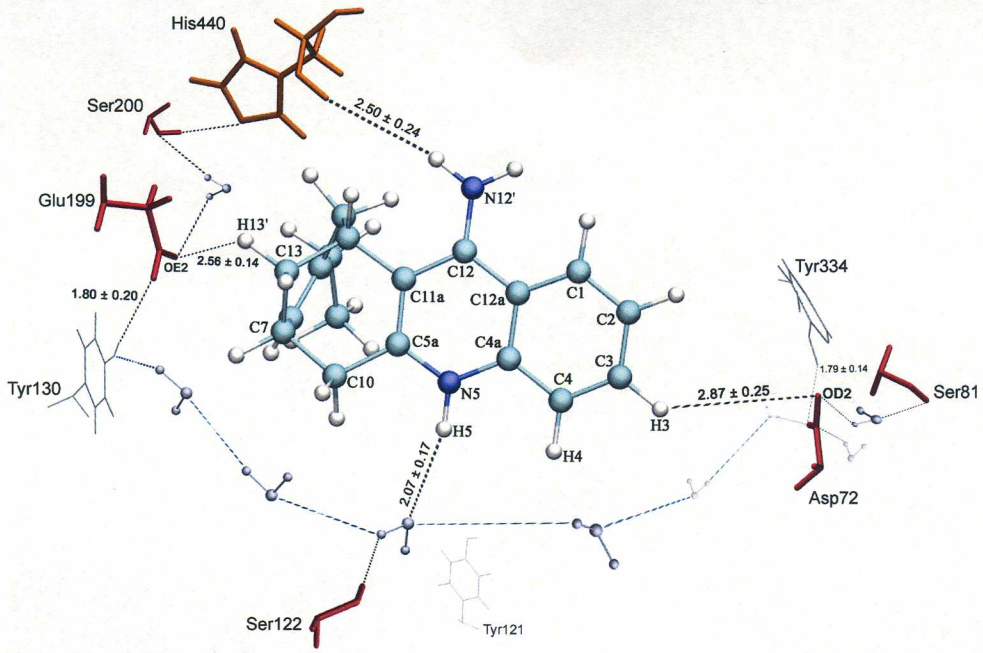
His440
Ser200
2.50 ± 0.24
Glu199
N12'
H13'
C13
OE2
2.56 ± 0.14
C12
C11a
C12a
C1
C2
C7
C5a
C4a
C3
C10
N5
C4
H5
H3
H4
1.80 ± 0.20
Tyr130
Tyr334
1.79 ± 0.14
Ser81
2.87 ± 0.25
OD2
2.07 ± 0.17
Asp72
Ser122
Tyr121

(a)

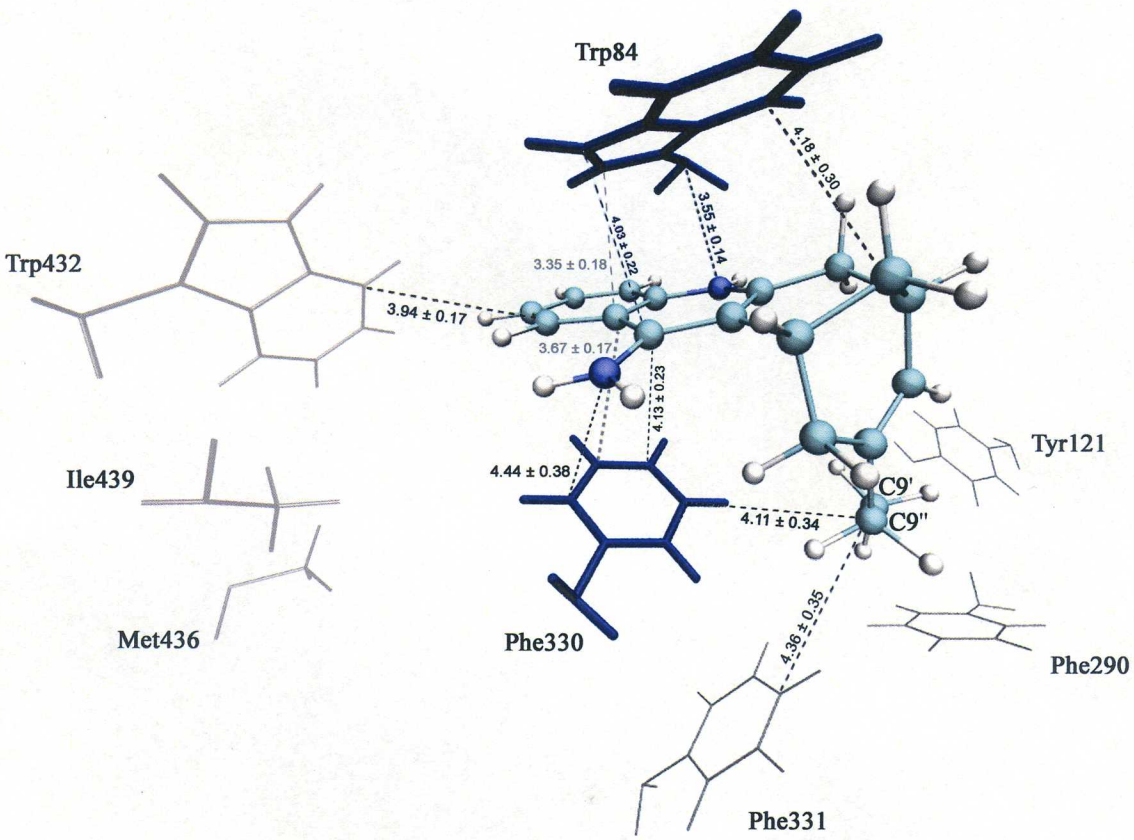
Trp84
4.18 ± 0.30
3.55 ± 0.14
4.03 ± 0.22
3.35 ± 0.18
Trp432
3.94 ± 0.17
3.67 ± 0.17
4.13 ± 0.23
Tyr121
Ile439
4.44 ± 0.38
C9'
4.11 ± 0.34
C9"
Met436
Phe330
4.36 ± 0.35
Phe290
Phe331

(b)

Figure 9